Permeation of Chlorinated Hydrocarbons Through Nylon 6/Ethylene–Propylene Rubber Blends

Soney C. George,[1] K. N. Ninan,[2] G. Geuskens,[3] Sabu Thomas[4]

[1]*Department of Basic Sciences, Amal Jyothi College of Engineering, Koovapally P.O., Kottayam 686518, India*
[2]*Propellant and Special Chemicals Group, PSC Division, VSSC, Thiruvananthapuram*
[3]*Department of Macromolecules, University of Brussels, Campus Plaine, CP 206-1, Boulevard du Triomphe, B-1050 Brussels, Belgium*
[4]*School of Chemical Sciences, Mahatma Gandhi University, Priyadarshini Hills P.O., Kottayam-686 560, India*

Received 18 February 2003; accepted 1 August 2003

ABSTRACT: Vapor transport offers one the unique ability to study structure–property relationships in polymers. An analysis of the transport of chlorinated hydrocarbons through nylon/ethylene–propylene rubber (EPR) blend membranes showed us how the permeation behavior varied according to the structure and morphology of the material under study. Binary blends were subjected to solvent transport studies. The solvent uptake increased with EPR content and decreased with nylon content. The behavior varied with the blend morphology. The effects of blend ratio, compatibilization, and dynamic vulcanization on the vapor permeation behavior of nylon/EPR blends were investigated in detail. The results from the vapor permeation studies were complimentary to those of the morphology studies. © 2004 Wiley Periodicals, Inc. J Appl Polym Sci 91: 3756–3764, 2004

Key words: nylon; rubber; blends

INTRODUCTION

Vapor permeation has emerged as a new industrial membrane technology. In vapor permeation, the transport of a condensable vapor through a dense membrane consecutive to an activity gradient takes place. This process offers one the unique ability to study the transport process of a single permeant through a dense membrane under various upstream activities.[1] Such characteristics can by no means be obtained by liquid permeation (pervaporation), where the modification of the upstream activity of a component can only be achieved by the addition of another compound to the mixture; the activity of both components is modified in this case in compliance with the Gibbs–Duhem relation, which complicates the transport analysis. On the contrary, coupling phenomena are not to be considered with pure vapor permeation results. In the case of pure permeation, the upstream activity can easily be calculated if the upstream pressure is precisely monitored.[2]

In addition to these advantages, a study of solvent vapor permeation offers direct practical conclusions for the understanding and rational design of volatile organic compounds (VOCs) and vapor recovery from contaminated air streams.[3,4] Vapor permeation also offers significant opportunities for energy saving and solvent reuse compared to classical VOC control processes, such as incineration, oxidation, and active carbon absorption.

In addition to these advantages, the vapor sorption technique is a good tool for the thermodynamic characterization of polymer blends.[5,6] The analysis of the equilibrium sorption of a vapor by a blend can provide information on polymer–polymer interactions. The amount of vapor sorbed is related to its interaction with the blend. The usual technique for investigating the morphology of an immiscible polymer blend is scanning electron microscopy (SEM) applied to the surface of cryofractures. However, that technique gives a picture of only a minute portion of the sample, which is sometimes nonrepresentative of the bulk of the material. Moreover, from a two-dimensional picture, it is not easy to estimate when phase inversion occurs as a function of composition and when the level of phase cocontinuity reaches a maximum.

Nylon 6 is an engineering thermoplastic characterized by its high tensile strength, impact strength, toughness, rigidity, abrasion resistance, and resistance to hydrocarbons. It is used mainly in engineering applications. Ethylene–propylene rubber (EPR) is a specialty rubber characterized by excellent aging and weathering resistance. Blends of nylon and EPR are a new class of thermoplastic elastomers that combine the excellent processability characteristics and engineering properties of nylon 6 and the elastic and ozone-resistance properties of EPR. These blends ex-

Correspondence to: S. C. George (soneygeo@sancharnet.in).

Journal of Applied Polymer Science, Vol. 91, 3756–3764 (2004)

hibit excellent impact properties and lower water absorption characteristics. However, these blends are incompatible, with poor physical and chemical interactions across the phase boundaries. Hence, this system requires compatibilization to improve its properties. The effect of maleic anhydride (MA)-modified EPR as a compatibilizer on the properties of nylon/EPR blends was investigated recently. Thomas et al.[7] reported the effect of blend composition and morphology on the transport behavior of nylon 6/EPR membranes.

In this study, we examined the effects of the blend ratio, compatibilizer addition, and dynamic vulcanization on the vapor permeation of chlorohydrocarbons through nylon/EPR blends. In addition, we used the permeation results to complement the observations from SEM. The solvent transport through EPR/nylon binary blends was also investigated.

EXPERIMENTAL

Materials

Nylon 6 [weight-average molecular weight (M_w) = 24,000] was supplied by DSM (Netherlands). It was dried at 120°C for 12 h before blending. EPR (M_w = 80,000), with a 78% ethylene content, was supplied by Exxon Chemical Co. EPR-*g*-MA (0.6 wt % of MA) was also supplied by Exxon Chemical. The solvents CH_2Cl_2, $CHCl_3$, and CCl_4 were used without further purification.

Blend preparation

Blends were prepared in a corotating twin-screw batch-type mini-extruder (DSM) under a nitrogen atmosphere. The mixing time, temperature, and rotor speed were 10 min, 250°C, and 100 rpm, respectively. The different composition used in this study were E_0, E_{30}, E_{50}, E_{70}, and E_{100}, where the subscript represents the weight percentage of EPR in the blend. For the comptatibilized blends (E_{30}), the compatibilizer concentration was varied from 1 to 20 wt %. The dynamic vulcanization of the nylon/EPR (50/50) blend was done with 3,4-dimethyl-3,4-diphenyl hexane (DDH; Perkadox 58) and 1,6-diamine hexane (DH; Fluka 33000) as vulcanizing agents. The dosages of the curing agent in both cases were 2 and 4 phr (parts per hundred rubber).

Blend morphology

A scanning electron microscope was used to study the phase morphology of the blends. The samples were fractured under liquid nitrogen, and one of the phases was suitably extracted. Blend samples with dispersed EPR phases were extracted with boiling xylene for 12 h. At higher EPR concentrations, nylon was extracted with formic acid. The dried samples were sputter-coated with gold before SEM examination. A Philips model scanning electron microscope operating at 10 kV was used to view the specimens.

Vapor permeation studies

The vapor permeability was determined at room temperature by measurement of the weight loss of small vials filled with solvents and tightly closed by a membrane 150 μm thick. The weight loss was proportional to the time, area of the membrane, and pressure inside the vials and was inversely proportional to the thickness of the membrane.

Swelling measurements

Circular samples were punched out from the molded sheets with a sharp-edged steel die ($\approx$ 1.96). The thickness of the samples was measured at several points with an accuracy of $\pm$0.001 cm with a micrometer screw gauge. Test samples were immersed in solvents in sorption bottles kept at a constant temperature in an air oven. They were taken out at regular intervals and weighed on an electronic balance (Shimadzu, Libror AEU 210, Japan) with an accuracy of $\pm$0.001 g. The weighing was continued until equilibrium was attained. The time for each weighing was kept to a minimum of 30–40 s to eliminate error due to the escape of solvent from the samples.

The sorption results were analyzed in terms of the moles of solvent sorbed [Q_t (mol %)] by 100 g of rubber. The Q_t value was determined as

$$Q_t \text{ (mol \%)} = \frac{\text{Mass of solvent sorbed by the sample}}{\text{Molar mass of solvent}} \times \frac{100}{\text{Initial mass of the polymer sample}} \quad (1)$$

The Q_t values obtained were plotted as functions of the square root of time.

RESULTS AND DISCUSSION

Vapor transport

Effect of the blend ratio

The permeation coefficients and sorption coefficients of nylon, EPR, and their blends are shown in Figure 1. The permeation coefficients and the sorption coefficients increased with increasing volume fraction of EPR in the blend. The permeation coefficient of nylon was small compared to that of pure EPR. The blend compositions had intermediate values. An increase in

permeability was observed after a 0.3 volume fraction of EPR. A clear hump was seen at a 0.5 volume fraction of EPR. The permeability and the sorption coefficients for nylon were much lower due to its inherent crystallinity. As the crystalline nylon phase decreased with increasing volume fraction of EPR, the sorption coefficient increased and so did the permeation coefficient. These observations supported the hetrophase structure revealed from the morphology. Figure 2 shows the morphology of the nylon/EPR blends. The SEM photographs showed that blends were heterogeneous in nature. In the E_{30} blend, EPR was dispersed as domains in the continuous nylon matrix. However, in the E_{50} blend, an interpenetrating morphology was observed. Here, both EPR and nylon formed a cocontinuous morphology. In the E_{70} blend, nylon was dispersed as domains in the continuous EPR matrix. The dispersed/matrix morphology of the E_{30} and E_{70} blends offered a more tortuous path for the penetrants and thereby reduced the permeability. However, the cocontinuous morphology of the E_{50} blend offered a smooth passage for the penetrants through the membrane, thereby increasing the permeability.

Investigation of blend morphology

The permeability of immiscible polymer blends depends on their morphology. Two extreme cases can be considered that correspond to the multilayers of the two components either parallel or perpendicular to the direction of the permeant flux. They can be described as fully continuous and fully discontinuous phase morphologies, respectively. The permeabilities of such systems vary with the permeabilities of the individual components (P_1 and P_2) and with their volume fractions (ϕ_1 and ϕ_2). If the continuous phase is more permeable, a parallel model represents the limiting behavior, which is given by the following equation:[8]

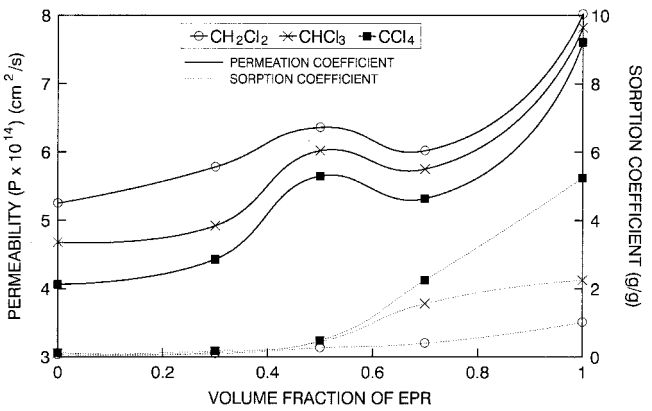

Figure 1 Variation of the permeation and sorption coefficients of nylon/EPR blends.

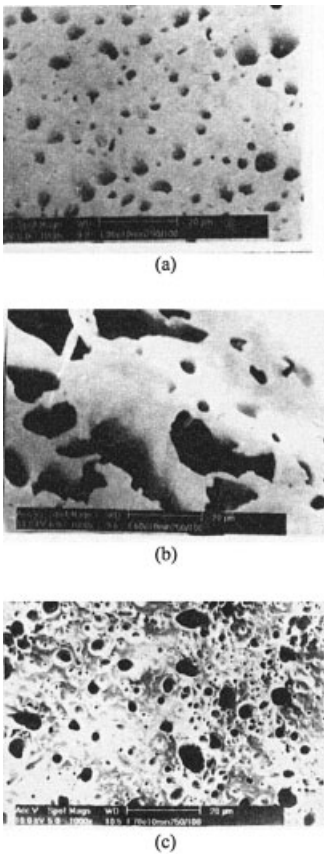

Figure 2 SEM photographs of nylon/EPR blends: (a) E_{30}, (b) E_{50}, and (c) E_{70}.

$$P = \phi_1 P_1 + \phi_2 P_2 \tag{2}$$

where P is the blend permeability. The series model in which the dispersed phase exhibits the greater permeability is represented by the following equation:[8]

$$1/P = \phi_1/P_1 + \phi_2/P_2 \tag{3}$$

A plot of permeability versus volume fraction shows an upward concavity for the parallel and a downward concavity for the series model (Fig. 3). In polymer blends with more complex morphologies, a change of concavity is also expected to occur with phase inversion when a dispersed phase becomes continuous and vice versa.

To describe the effect of a permeating component on the overall blend permeability, Maxwell suggested the following equation:[8]

$$P = P_m\left[\frac{P_d + 2P_m - 2\phi_d(P_m - P_d)}{P_d + 2P_m + \phi_d(P_m - P_d)}\right] \tag{4}$$

where ϕ is the volume fraction and the subscripts m and d refer to the continuous matrix phase and the dispersed phase, respectively.

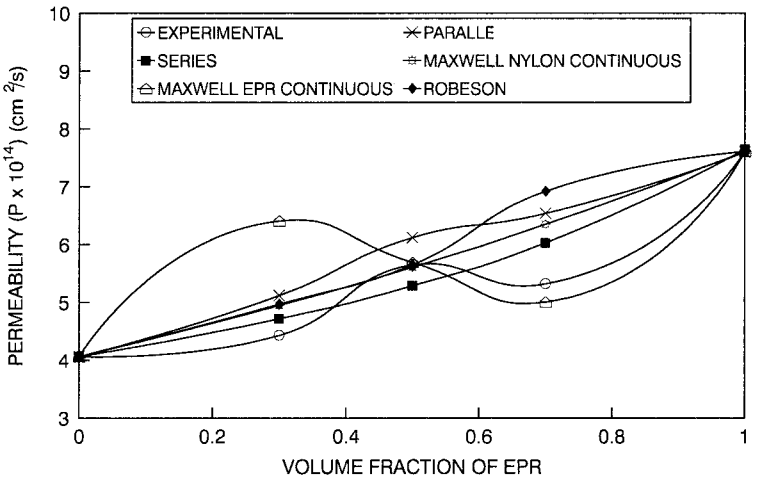

Figure 3 Comparison of experimental permeation results with theoretical models for nylon/EPR blends.

Robeson extended Maxwell's analysis by assuming that at intermediate concentrations, both phases contribute continuous and discontinuous characteristics. The addition of Maxwell's equations for both phases, weighted to their fractional contribution to the continuous phase results in[8]

$$P = X_a P_1\left[\frac{P_2 + 2P_1 - 2\phi_2(P_1 - P_2)}{P_2 + 2P_1 + \phi_2(P_1 - P_2)}\right] + X_b P_2\left[\frac{P_1 + 2P_2 - 2\phi_1(P_2 - P_1)}{P_1 + 2P_2 + \phi_1(P_2 - P_1)}\right] \quad (5)$$

where X_a represents the fraction of the composition in which component 1 is the continuous phase and X_b corresponds to a continuous phase of component 2. The description of such a cocontinuity is limited by the restriction that

$$X_a + X_b = 1 \quad (6)$$

A composition range in which the permeability data are described by $X_a = X_b$ can be taken as an indication of phase inversion. Figure 3 shows the experimental and theoretical curves of permeability of the nylon/EPR blends as a function of the EPR volume fraction. In the nylon/EPR blend with a 0.3 volume fraction of EPR, the permeability data was close to the series model. In the nylon/EPR blends, the highly permeating EPR formed the dispersed phase in continuous nylon matrix. Above a 0.3 volume fraction, there was an inflection point, and this indicated a phase inversion at this volume fraction. At a 0.5 volume fraction of EPR, the permeability of the blend coincided with Robeson's model, which is based on a cocontinuous morphology. Hence, at this volume fraction of EPR, the blend exhibited a cocontinuous morphology. Between a 0.5 and 0.7 volume fraction of EPR, there was another inflection point, which also indicated a phase inversion. At a 0.7 volume fraction of EPR, the permeability of the blend was close to that for the Maxwell model with the EPR continuous phase. This indicated that in the nylon/EPR blend with a 0.7 volume fraction of EPR, the EPR formed the continuous phase and the nylon formed the dispersed phase.

Effect of compatibilization

The addition of suitably selected compatibilizers to an immiscible binary blend should (1) reduce the interfacial energy between the phases, (2) permit finer dispersion during melt mixing, (3) provide stability against gross segregation, and (4) improve the interfacial adhesion.[9] Several experimental investigations have been reported on the compatibilizing action of added block and graft copolymers in heterogeneous blends.[10,11] Nylon was compatibilized with a second immiscible phase (EPR) by the introduction of a compatibilizer precursor (EPR-*g*-MA), which was physically miscible with the second phase but had a chemical functionality (MA group) that could react with the amino end group of nylon to form a graft copolymer at the interface, as shown in Figure 4. Graft copolymer formation has been reported by a large number of

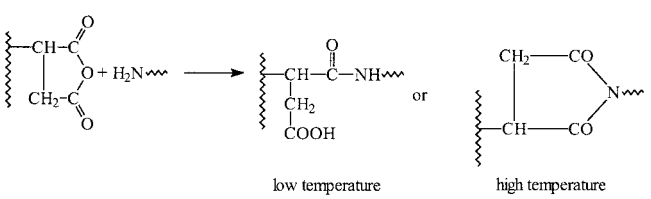

Figure 4 Schematic representation of the reaction between the amino end group of nylon and the MA group of EPM (EPM-*g*-MA).

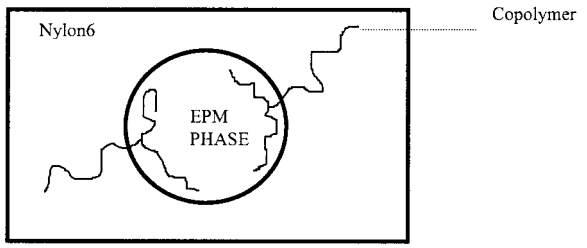

Figure 5 Schematic illustration of the conformation of the graft copolymer at the interface.

researchers, and the reaction between anhydride and the amino end group of nylon is well documented in the literature.[12–15] The idealized location of the graft copolymer is demonstrated in Figure 5, where the compatibilizer species was miscible with the EPR phase and had functional groups that were capable of forming linkages with the nylon chains at the interface. This situation was expected to lead to a reduction in particle size through a reduction in interfacial tension and an increased resistance to coalescence through the stabilization of the interface. The effect of EPM-*g*-MA as a compatibilizer on the permeability of the E_{30} blend is shown in Figure 6. With increasing weight percentage of compatibilizer, the permeability sharply increased, reached a maximum at 2.5 wt % compatibilizer, and then decreased. There was only a little change in the permeation coefficient values at a higher compatibilizer concentration. This behavior was directly associated with the morphology of compatibilized blends. From the SEM photographs (Fig. 7), we observed that the size of the dispersed EPR phase decreased with the addition of compatibilizers. This reduction in particle size with the addition of modified polymers was due to the reduction in interfacial tension between the dispersed EPR phase and the nylon matrix and also the suppression of coalescence.

The average size and total surface area of the EPR domains in the compatibilized blends as a function of

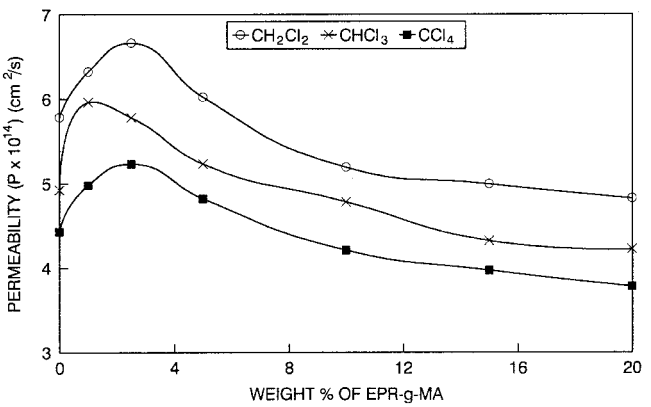

Figure 6 Effect of compatibilizer concentration (wt % of EPM-*g*-MA) on permeation coefficients.

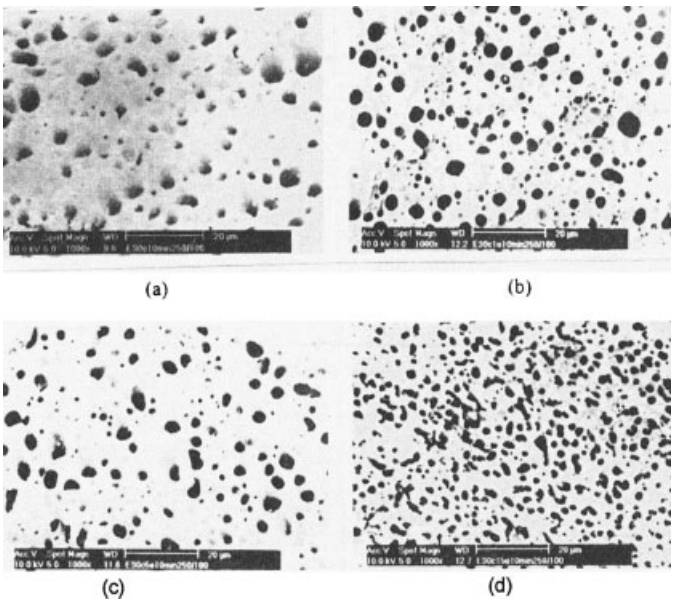

Figure 7 SEM photographs of uncompatibilized and compatibilized nylon/EPR blends: (a) uncompatibilized blend and (b) 1, (c) 5, and (d) 15 wt % of EPM-*g*-MA.

the compatibilizer concentration are shown in Figure 8. The average domain size of the unmodified blend was 3.5 μm. For the MA–EPM compatibilized blends, the addition of 1% of EPM-*g*-MA caused a change in domain size of 45.7%. The further addition of EPM-*g*-MA did not change the domain size considerably, and a leveling off was observed. The equilibrium concentration at which the domain size leveled off was considered as the so-called critical micelle concentration (cmc), that is, the concentration at which micelles were formed. The cmc was estimated by the intersection of the straight line at the low- and high-concentration regions. The cmc value for the EPM-*g*-MA

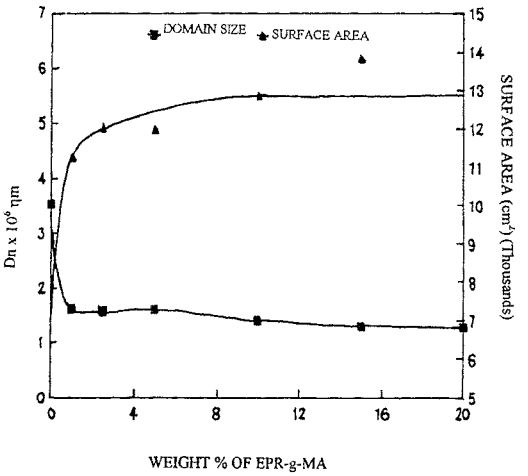

Figure 8 Variation of number-average domain size and surface area with compatibilizer concentration.

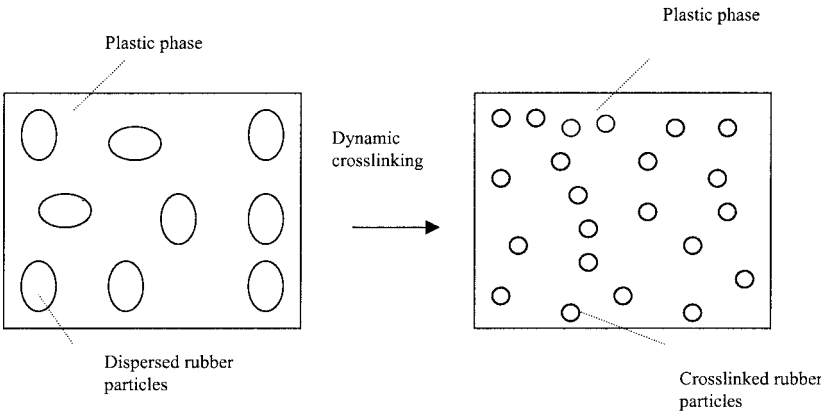

Figure 9 Schematic representation of the morphology of the dynamic vulcanized thermoplastic elastomer.

system in this blend was 2%. The cmc value indicated the critical amount of compatibilizer required to saturate the unit volume of the interface. Several authors reported on the interfacial saturation of binary polymer blends by the addition of compatibilizers.[16–18] Thomas and Prud'homme[18] reported that in polystyrene/poly(methyl methacrylate) at lower concentrations of the copolymer, the dispersed phase size decreased linearly with increasing copolymer concentration, whereas at higher concentrations, it leveled off. Interestingly, the total surface area increased sharply with increasing concentration of EPM-*g*-MA, and later, it leveled off. The increase in permeability with increasing weight percentage of compatibilizer up to 2 wt % was attributed to the increase in the total surface area, as shown in Figure 8. As the compatibilizer content was increased beyond 2%, the surface area was almost unaffected, whereas the interface adhesion kept increasing. This accounted for the decrease in permeability at higher compatibilizer contents beyond 2%.

Effect of dynamic vulcanization

The vulcanization of the rubber phase during mixing was as a method for improving the physical properties of several thermoplastic elastomers based on rubber/plastic blends. During dynamic vulcanization, the crosslinked rubber phase became finely and uniformly distributed in the plastic matrix and attained a stable morphology, as shown schematically in Figure 9.

In this study, two vulcanizing agents were used. These were DDH and DH. Both introduced C—C bonds between the rubber chains. The variation in the permeability of the E_{50} blend crosslinked with DDH and DH is shown in Figure 10. It is very clear from Figure 10 that permeability decreased with crosslinking. The effect of the concentration of crosslinking agent is also shown in Figure 11. With increase in the concentration of both of the crosslinking agents from 0

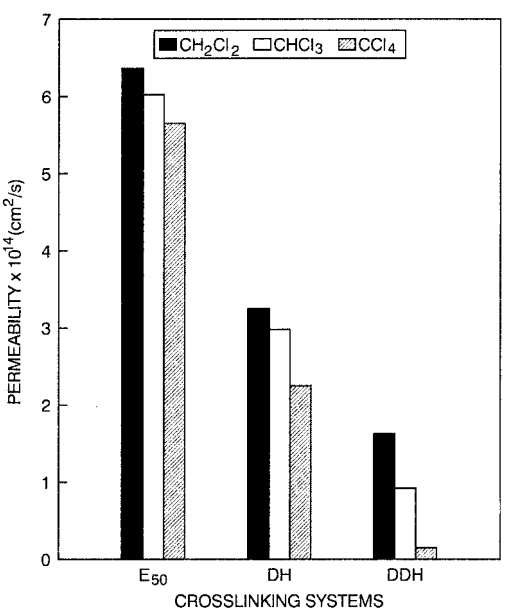

Figure 10 Variation of permeability with different crosslinking systems: E_{50} was uncrosslinked, DH–E_{50} was crosslinked with DH, and DDH–E_{50} was crosslinked with DDH.

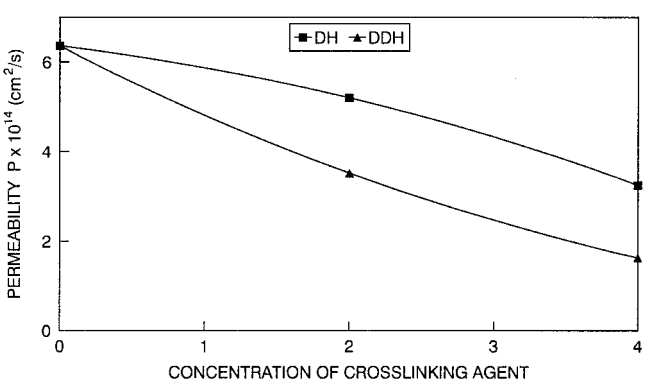

Figure 11 Variation of permeability with concentration of crosslinking agent (phr): E_{50} was uncrosslinked, DH–E_{50} was crosslinked with DH, and DDH–E_{50} was crosslinked with DDH.

TABLE I
$\nu \times 10^3$ (mol/cc)

Sample	$\nu \times 10^3$
E_{50}	2.11[a]
DH_2[b]	2.19
DH_4	2.25
DDH_2[c]	2.43
DDH_4	2.75

Subscripts 2 and 4 stand for the dosage of the curing agent.
[a] Due to physical entanglements.
[b] 1,6-Diamine hexane.
[c] 3,4-dimethyl-3,4-diphenyl hexane.

to 4 phr, the permeability decreased. This difference in behavior could be explained on the basis of the crosslink density of the vulcanized samples. The degree of crosslinking (ν) was determined by the following relation:

$$\nu = 1/2M_c \quad (7)$$

where M_c is the molecular weight between crosslinks. M_c can be calculated with Flory–Rehner relation:

$$M_c = -\rho_p V_s \phi^{1/3}/(\ln(1-\phi) + \phi + \chi\phi^2] \quad (8)$$

where ρ_p is the density of the polymer, V_s is the molar volume of the solvent, ϕ is the volume fraction of the swollen rubber, and χ is the interaction parameter. The ν values are given in Table I. It is clear from the table that ν was at a minimum for the E_{50} blend (physical entanglements) and at a maximum for the DDH crosslinked samples. As ν increased, the sorption coefficient and diffusion coefficients decreased and, hence, the permeation coefficients decreased. With increasing concentration of crosslinking agent, the crosslinking density increased. Therefore, the rubber phase was tightly crosslinked, and hence, the permeability was highly reduced. The results obtained from the permeability studies were in agreement with the results from the morphology studies. The morphologies of the unvulcanized and vulcanized E_{50} blend are shown in Figure 12. On dynamic vulcanization, the cocontinuous morphology could be transformed into a matrix/dispersed phase morphology. This is clearly shown in Figure 12(a,b). With increasing extent of crosslinking, the domain size of the dispersed phase decreased, and this directly influenced the permeation behavior. The transformation of the morphology from a cocontinuous to a dispersed phase reduced the permeability. The SEM photographs of the DDH_2 [Fig. 12(c)] and DH_2 [Fig. 12(d)] vulcanized blends revealed that they exhibited a partial cocontinuous morphology and, thereby, had only a slight reduction in overall permeability.

Liquid transport

The sorption behavior of binary blends in CCl_4 is shown in Figure 13. It is clear that the solvent uptake increased rapidly from E_{30} to E_{70}. The sorption behav-

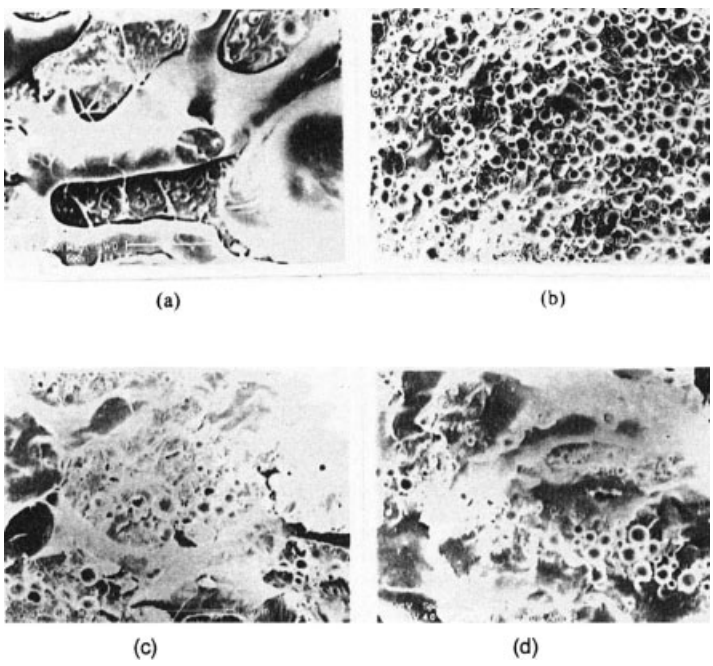

Figure 12 SEM photographs of unvulcanized and dynamically vulcanized E_{50} blends: (a) unvulcanized E_{50} blend, (b) DH (4 phr), (c) DDH (2 phr), and (d) DH (2 phr).

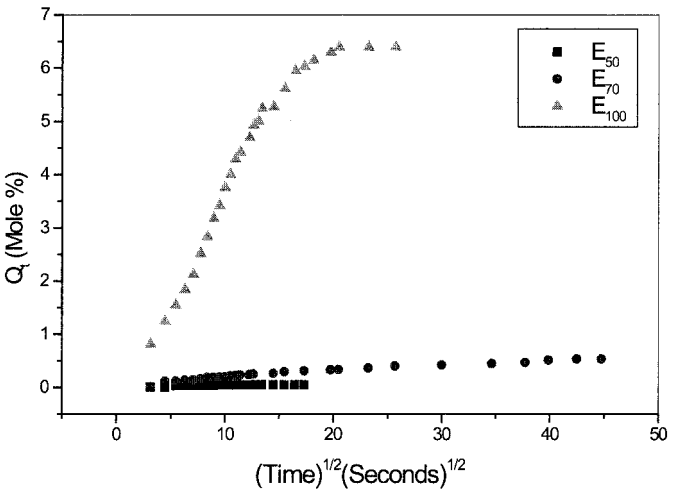

Figure 13 Transport behavior of nylon/EPR blends in CCl_4 at room temperature.

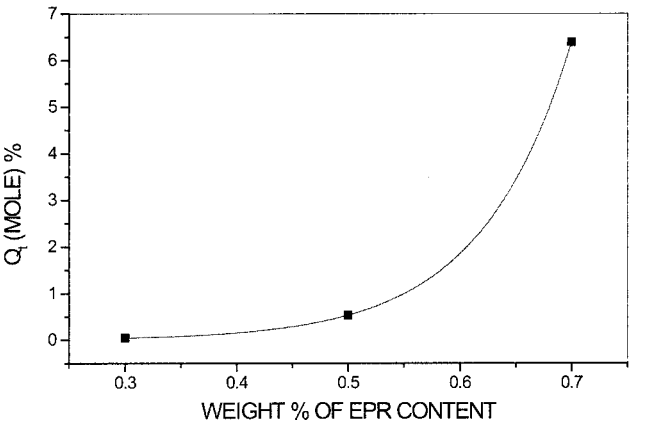

Figure 14 Variation of the maximum solvent uptake with weight percentage of EPR.

ior of E_0 (pure nylon) and E_{100} (pure rubber) are not shown here. This is because E_0 did not exhibit any solvent uptake, and E_{100} was not stable in a chlorohydrocarbon atmosphere. The solvent resistant behavior of nylon (E_0) could be explained on the basis of its inherent crystallinity. The crystallites and crystalline regions in nylon act as hindrance to the incoming solvent. Pure EPR (E_{100}) dissolved in the solvent due to the close proximity between the solubility parameter of EPR and carbon tetrachloride. Additionally, EPR rubber was amorphous; therefore, the hydrocarbon interacted strongly with EPR.

The sorption characteristics could be very well explained on the basis of blend morphology. Morphology has a significant influence on the permeation properties of polymer blends. The morphology of the nylon/EPR blends was already discussed and is shown in Figure 2. A shown in Figure 2, in E_{30}, EPR was dispersed as domains in the continuous nylon matrix. Because the nylon was the continuous phase, it restricted the solvent transport.

In E_{50}, both nylon and EPR phases interpenetrated to give a cocontinuous morphology, as described earlier. In the cocontinuous morphology, transport took place through the contours of the EPR phase from the continuous nylon matrix. An inversion of morphology occurred at E_{70}. In this blend, nylon was dispersed in the continuous EPR matrix. Therefore, the solvent transport was accelerated. Thus, the increase in rubbery content, decrease in crystallinity from E_{30} to E_{70}, and morphological changes contributed to the sorption behavior of the nylon/EPR blends.

Figure 14 shows the variation of maximum solvent (Q_∞) with increasing weight percentage of the EPR phase. With increasing rubber content, the maximum solvent uptake also increased. The slope of the curve showed a dramatic change when the rubber content was more than 50%, where it became a continuous phase. Transport was also affected by the crystallinity of the blends. Because the addition of rubber decreased the crystallinity of the samples, the transport process was accelerated.

Concentration dependency of diffusion

With the Joshi–Astarita model,[19] the diffusivity values are presented as a function of the solvent concentration of the nylon/EPR blends at room temperature, as shown in Figure 15. Concentration-dependent diffusivity arose from the presence of solvent molecules within the polymer, which weakened the interaction between adjacent polymer chains. In the case of E_{50} and E_{70}, the diffusivity increased with increasing penetrant concentration, reached a maximum, and then

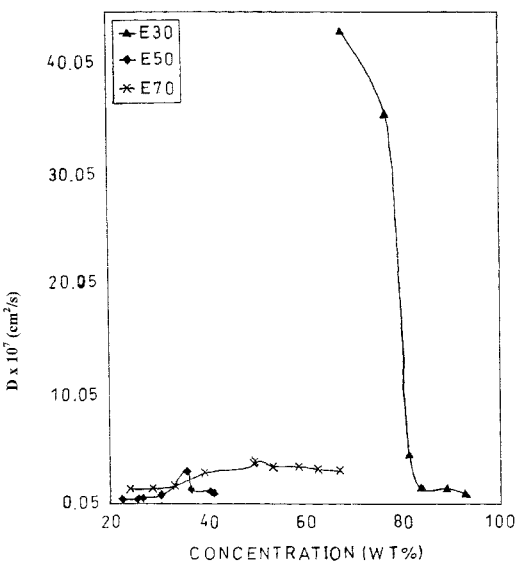

Figure 15 Variation of diffusivity with penetrant concentration.

decreased. The E_{50} sample showed sharp maxima, whereas E_{70} showed broad maxima. This suggests that the E_{50} sample was more concentration dependent. Penetrant concentration present in either of the cases at maxima indicated the capacity of the polymer matrix to accommodate solvent molecules in similar conditions. The importance of the concentration dependence of *D* was clear from the magnitude of change in *D* for small increases in penetrant concentration. Diffusivity decreased with increasing penetrant concentrations for the E_{30} system.

CONCLUSIONS

Transport of chlorinated hydrocarbon vapors through nylon, EPR, and their blends showed that the permeation process was influenced by the blend ratio, compatibilization, and dynamic vulcanization. The permeation coefficient values increased with EPR concentration in the blend. However, when the different blend compositions were compared, we observed that the E_{30} blend had the lowest permeation coefficient value and E_{50} had the highest. This behavior was attributed to the dispersed/matrix phase morphology of the E_{30} blend and the cocontinuous nature of the E_{50} blend, respectively. Comparison of the experimental permeability data with theoretical predictions confirmed the cocontinuous nature of the E_{50} blend.

Compatibilization also had a significant influence on permeation behavior. The permeation coefficient values increased with compatibilizer concentration up to the cmc and then decreased. At higher compatibilizer concentrations, the permeation coefficient values showed a leveling off. This behavior was attributed to the increase of total surface area by the addition of compatibilizer, and it leveled off at higher compatibilizer concentrations. The investigation of permeability data in the dynamically vulcanized E_{50} blend showed that the permeation coefficient decreased with increasing concentration of crosslinking agent. The crosslinker DDH was more active than DH. Permeability decreased in the following order: uncrosslinked $E_{50} > E_{50}$ crosslinked with DH $> E_{50}$ crosslinked with DDH. This was associated with the difference in crosslink densities in the various systems. In fact, on dynamic vulcanization, the cocontinuous morphology of E_{50} was transformed into a partial cocontinuous morphology at lower concentrations of crosslinking agent and was fully converted into a dispersed/matrix morphology at higher concentrations of crosslinking agent. The transport of chlorohydrocarbon liquids through the nylon/EPR blends varied with rubber content, crystallinity, and blend morphology. Concentration-dependent diffusivity was observed for blends having a 50/50 composition.

References

1. Rogers, C. E.; Stanett, V.; Szwarc, M. J Polym Sci 1960, 45, 61.
2. Bitter, J. G. A. Transport Mechanism in Membrane Separation Systems; Plenum: New York, 1991.
3. Peinemann, K. V.; Mohr, J. M.; Baker, R. W. AIChE Symp Ser 1985, 250, 19.
4. Baker, R. W.; Yoshioka, N.; Mohr, J. M.; Khan, A. J Membr Sci 1987, 31, 259.
5. Kwei, T. K.; Nishis, T.; Roberts, R. F. Macromolecules 1974, 7, 667.
6. Gillberg, G.; Sawyer, L. C.; Promislow, A. L. J Appl Polym Sci 1985, 28, 3723.
7. George, S. C.; Groeninckx, G.; Ninan, K. N.; Thomas, S. Polymer 2000, 38, 2136.
8. Hopferberg, H. B.; Paul, D. R. In Polymer Blends; Paul, D. R.; Newman, S., Eds.; Academic: New York, 1978; Chapter 10.
9. Paul, D. R.; Barlow, G. W. Adv Chem Ser 1979, 176, 315.
10. Asaletha, R.; Kumaran, M. G.; Thomas, S. Rubber Chem Technol 1995, 68, 671.
11. Brahimi, B.; Ait-Kadi, A.; Ajji, A.; Fayt, R. J Polym Sci Part B: Polym Phys 1991, 29, 946.
12. Avella, M.; Greco, R.; Lanzetta, N.; Maglio, G.; Malinconico, M.; Martusscelli, E.; Palumbo, R.; Ragosta, G. In Polymer Blends: Processing, Morphology and Properties; Plenum: New York, 1980.
13. Amelino, L.; Cimmino, S.; Greco, R.; Lanzetta, N.; Maglio, G.; Malinconco, M.; Martuscelli, E.; Palumbo, R.; Silvestre, C. Polymer Blends, Preprints of Plasticon 81, Warwick, England, 1981.
14. Avella, M.; Lanzetta, N.; Maglio, G. M.; Malinconico, M.; Musto, P.; Palumbo, R. Preprints of the 2nd Joint Polish Italian Seminar on Multicomponent Polymeric Systems, Lodz, Poland, 1981.
15. Cimmino, S.; D'orazio, L.; Greco, R.; Maglio, G.; Malinconico, M.; Mancarella, C.; Martuscelli, E.; Palumbo, R.; Racosta, G. Polym Eng Sci 1984, 24, 48.
16. Spiros, H. A.; Irena, G.; Koberstein, J. T. Macromolecules 1989, 22, 1449.
17. Fayt, R.; Jerome, R.; Teyssie, P. Makromol Chem 1986, 187, 837.
18. Thomas, S.; Prud'homme, R. E. Polymer 1992, 33, 4260.
19. Joshi, S.; Astarita, G. Polymer 1979, 20, 455.